

Nanoscale

Accepted Manuscript



This is an *Accepted Manuscript*, which has been through the Royal Society of Chemistry peer review process and has been accepted for publication.

Accepted Manuscripts are published online shortly after acceptance, before technical editing, formatting and proof reading. Using this free service, authors can make their results available to the community, in citable form, before we publish the edited article. We will replace this *Accepted Manuscript* with the edited and formatted *Advance Article* as soon as it is available.

You can find more information about *Accepted Manuscripts* in the [Information for Authors](#).

Please note that technical editing may introduce minor changes to the text and/or graphics, which may alter content. The journal's standard [Terms & Conditions](#) and the [Ethical guidelines](#) still apply. In no event shall the Royal Society of Chemistry be held responsible for any errors or omissions in this *Accepted Manuscript* or any consequences arising from the use of any information it contains.

**Electronic transport regimes through an alkoxythiolated diphenyl-2,2'-bithiophene-based
molecular junction diodes: critical assessment of the thermal dependence**

Giuseppina Pace^{a,}, Lorenzo Caranzi^{a,b}, Sadir Bucella^{a,b}, Eleonora V. Canesi^c, Giorgio
Dell'Erba^{a,b}, Chiara Bertarelli^c, Mario Caironi^{a,*}*

^a Center for Nano Science and Technology@PoliMi, Istituto Italiano di Tecnologia, Via Pascoli
70/3, 20133 Milano, Italy

^b Dipartimento di Fisica, Politecnico di Milano, P.za L. Da Vinci, 32 20133 Milano, Italy

^c Dipartimento di Chimica, Materiali e Ing. Chimica, Politecnico di Milano, P.za L. Da Vinci, 32
20133 Milano, Italy

Corresponding authors: (G. P.) giuseppina.pace@iit.it; (M. C.) mario.caironi@iit.it.

Abstract

The detailed understanding of electronic transport through a single molecule or an ensemble of self-assembled molecules embedded between two metallic leads is still a matter of controversy. Multiple factors influence the charge transport in the molecular junction, with particular attention to be given to the band states of the electrodes, molecular orbital energies, bias potential and importantly molecule-electrodes electronic coupling. Moreover it is not trivial to disentangle molecular contributions from other possible conduction pathways directly coupling the opposite electrodes. We here investigate the electronic transport properties of an *ensemble* molecular junction embedding an alkylthiol derivative of a diphenol substituted bithiophene (DPBT) by means of current vs. voltage and temperature dependent measurements. We explored different junction configurations using: micropores (Au// DPBT //Au and Au// DPBT -polymer conductor//Au) and conductive-Atomic Force Microscopy (c-AFM). In all

cases, we found a transition voltage, V_T of ~ 0.35 V. The consistent presence of a similar V_T in all tested configurations is a strong, yet not conclusive, indication of a molecular signature in the charge transport, which we assessed and confirmed by temperature dependent measurements. We found a transition from incoherent resonant tunneling at low biases and close to room temperature, where transport is thermally activated with activation energy of ~ 85 meV, to a coherent tunneling at voltages higher than V_T . Unlikely many other molecular junctions reported in the literature, resonant conditions commonly attributed to a hopping transport regime can be found already at room temperature and very low biases for a molecule only ~ 1.5 nm long. This is the first report clearly showing temperature activated transport through a short and not fully conjugated molecule. Moreover, we could clearly identify a regime at low temperatures and low bias where the transport mechanism is controlled by the thermal conductivity of the metal electrodes rather than the molecule.

Introduction

The wide flexibility in tailoring the optoelectronic properties of organic materials has justified the efforts for their integration into electronic circuits for technology application. Molecular electronics studies are motivated by the promise for future electronics being based on single molecules or ensemble of molecules, providing one possible answer for extreme downscaling requirements needed to satisfy the ever increasing demand for denser computational capability.¹ Self-assembly of functional molecules and their tunable chemical composition may also provide a mean to deploy complex logic functionalities at the nanometer scale, through a unique and efficient bottom-up approach, thus enabling alternative applications not accessible with current technologies.² In order to achieve these targets, fundamental properties of molecular

junctions have to be investigated. Most of the current studies focus on conductive Atomic Force Microscopy (c-AFM) measurements^{3,4} and the break junction approach.⁵ These junction configurations enable very important fundamental studies, but they are still far from being suitable for the following step of integration into a scaled-up technology. Furthermore, the transport properties so far investigated with the break junction technique are strongly correlated to the particular atomic configuration of the apex metal contacts, and the effectiveness of controlling the alignment of a single molecule between them. A more scalable design is based on ensemble molecular junction diodes, where many self-assembled molecules are sandwiched between two electrodes.⁶ Various examples of ensemble molecular junctions can be found in literature, and most of them exploit the self-assembling properties of thiolated molecules bound to gold electrodes.^{6b} Typical artifacts encountered in the electrical characterization of molecular junctions are caused by metal diffusion filaments formed during the thermal evaporation of the top metal contact.⁷ Unfortunately, the electronic conductivity of those filaments has been often misinterpreted and assigned to molecular charge transport features.⁸ More recent strategies foresee the development of soft electrode deposition methods.⁹ A valuable approach is the insertion of a protective poly(3,4-ethylenedioxythiophene) poly(styrenesulfonate) (PEDOT:PSS), acting as a conductive interlayer, between the self assembled monolayer (SAM) and the thermally evaporated top metal contact.¹⁰ Other works have also shown the effectiveness of using graphene and graphene oxides as soft contacts.¹¹ Once the diode configuration is defined, the junction transport properties have to be rationalized in light of the specific adopted architecture and molecular features have to be extrapolated.

The typical transport mechanisms often showed in a molecular junction are tunneling and resonant transport.¹² A non resonant tunneling mechanism, which is temperature independent, is

avored in the case of thin monolayer and high energy offset between molecular orbitals energy and electrodes work function. Resonant transport mostly occurs when the molecule's HOMO or LUMO are involved into the electronic transport through the electrode-molecule electronic coupling. In particular, the charge hopping mechanism operates in resonant conditions and features an Arrhenius dependence of the conductivity versus temperature. Non resonant tunneling has been previously found to dominate for chain length shorter than 2.5 nm even for fully conjugated molecular wires.¹³ For these molecules a hopping mechanism is more likely to occur when the chain length is longer than 5 nm.¹⁴ So far it is not clear if a hopping mechanism can be achieved for short and not fully conjugated systems.

In this work we present ensemble molecular junctions based on an alkoxythiolated 3,3'-diphenyl-2,2'-bithiophene (DPBT), which is designed to embed insulating alkyl chains in between the electrodes and the aromatic core. Multiple techniques have been employed in this study to unveil a molecular fingerprint in the electrical conduction, namely the robustness of the electrical parameters extracted with different junction architectures comprising the same DPBT molecule. In particular, c-AFM allows for an easier fabrication and a wider junction's statistic with respect to the case of pore-junctions. Therefore, our study foresees the use of c-AFM as a first technique, which allows us to identify from the current-voltage (I - V) measurements a precise transition voltage (V_T), which is found as a minimum in the transition voltage plot, where the usual I - V data are plotted in a Fowler Nordheim (FN) manner (i.e., $\ln(I/V^2)$ vs $1/V$).¹⁵

The study then moves to the I - V characterization of a large number of micro-pore junctions with and without the PEDOT:PSS soft-contact. In both cases we found the same V_T as for c-AFM measurements, highlighting the critical role of the molecule in determining the junction transport characteristics independently from the top contact. Variable temperature I - V

curves acquired on micro-pore junctions allow the proper investigation of the transport mechanism. Importantly, we were able to evidence a clear agreement between variable temperature measurements on pore junctions with both top Au and PEDOT:PSS contacts. This is a critical finding, further confirming the specific role of the molecule in determining charge transport. Therefore, by combining different characterization techniques and by a critical assessment of the thermal dependence of the current-voltage (I - V) characteristic curves, we found that resonant transport can be achieved also for such short and not fully conjugated chain. We show that by the proper design of the Highly Occupied Molecular Orbital (HOMO) level, being very close to the gold work function, and by inserting a short insulating alkyl chain between the metal and the aromatic core, we could enable a thermally activated transport regime at low biases and at room temperature implying the contribution of the conjugated core of the molecule.

Results

The molecule under study (DPBT, Figure 1) has an aromatic core and two insulating saturated alkyl chains constituted by six carbon atoms, one of which terminated with a thiol group. The aromatic core determines its HOMO and LUMO, whose energies have been measured through Cyclic Voltammetry (CV, Figure S1 Supporting Information, SI). A DPBT monolayer was grown on a gold surface thanks to its anchoring $-SH$ group, according to the methodology reported in the Methods section, and its presence was shown by grazing angle incidence Reflection Absorption Infrared Spectroscopy (RAIRS) data (Figure S2 and Table 1 in SI).

We first investigated the conduction through such monolayer by means of c-AFM technique, i.e. by adopting the conductive tip of an AFM as the counter probing electrode.

I-V measurements were performed at room temperature and under N₂ atmosphere. The collected data are reported in Figure 2a and c, and compare c-AFM junctions containing saturated tetradecanethiol (C14) SAMs or DPBT SAMs chemisorbed on gold. C14 based junctions have been selected as reference samples since C14 chain length is comparable to the DPBT one. Per each molecule at least four freshly made SAM samples were characterized. Per each SAM at least three different sampling points were tested. The data presented are averaged over at least 20 *I-V* curves acquired per each tip load per testing point (raw data shown in Figure S3). We also present the data as a function of the applied load.¹⁶ The lowest currents are measured by applying the minimum load necessary to make the first electrical contact to the SAM. For DPBT the higher load is the one preceding the SAM rupture, favoring a short circuit through the junction. As shown in Figure 2, for similar tip loads the current intensities measured on C14 and DPBT (58 nN and 50 nN respectively) can be very different. Such differences may arise from a combined effect of different intrinsic conductivity and different mechanical properties of the two investigated SAMs due to the different packing and moisture adlayer, which affects the effective load to be applied for establishing the electrical contact to the SAM.

Though it has raised some controversy with respect to its proper interpretation, a useful tool to monitor the electrical characteristics of molecular junctions, is the extrapolation of the transition voltage V_T from the FN plot of *I-V* characteristics.^{15,17} The theoretical concept behind this plot is the Simmons model,¹⁸ which identifies in the V_T the voltage threshold for the transition between a direct tunneling to a Fowler Nordheim tunneling. However, care must be taken when assigning the minimum in the V_T plot to a transition between these or other specific

mechanisms.¹⁹⁻²⁰ Vilan and Cahen analyzed different tunneling transport models and have shown that such minima can also be found when a Taylor expansion is used to introduce small perturbation on one single tunneling mechanism, therefore no transition between two different transport mechanisms would be needed to observe a V_T .²¹

Keeping in mind all the above, the I - V data measured for molecular junctions in a c-AFM configuration are presented for comparison also in the form of transition voltage plots (Figure 2b and d). By comparing the I - V curves for both DPBT and C14 samples at very low applied loads, where the current intensity measured for the two junctions is similar, we can clearly see that a V_T (~ 0.35 V) appears only for the DPBT SAM, while is absent for the C14 one. Interestingly, the measured V_T for the DPBT junction is even lower than the one found for very short alkyl chains, as for example for a C8, where a V_T of ~ 0.5 V was reported for high tip loads.²² Also we observe that a persistent V_T is found for the entire range of applied loads for DPBT, contrarily to the C14 SAM. With increasing tip-load, V_T for DPBT stays almost constant at around $V_T = (0.32 \pm 0.03)$ V, while a jump to higher values occurs only for a tip-load closer to conditions of short circuiting of the diode (~ 0.5 V at 57 nN). From such analysis we observe that, besides showing a higher conductivity (Figure 2), DPBT junctions display a V_T which cannot be reproduced with a saturated carbon chain of similar and even shorter length. It is worth here to underline that our measurements on the reference C14 samples are consistent with previous reports on long alkyl chains, showing a V_T higher than 1V,²³ at the limit of our bias window. Within this window we could observe a V_T at around ~ 0.7 V only for high tip loads and only for few (10%) C14 junctions. Such decrease in V_T was previously shown for alkanethiols and assigned to a different tilting angle of the alkyl chains with respect to the substrate thus enabling different pathways for the charges to tunnel through the SAM.²² Such behavior is highly reproducible and implies that

in c-AFM the applied tip load can play a major role in determining the transport properties of a junction, reflected by the overall current density and V_T .¹⁶

We then compared the c-AFM junctions characteristics with the one found in pore junction diode configurations. A sketch of all the three different diode configurations investigated in this study is presented in Figure 3: i- Au//DPBT//Au; ii- Au//DPBT/PEDOT:PSS//Au; iii- Au//DPBT//(Pt, c-AFM tip). Here, we would like to point out that the data presented are the outcome of over a thousand investigated pore junctions with and without the soft PEDOT:PSS electrode. In spite of the very low yield in fabricating Au//DPBT//Au diode junction ($\sim 3\%$), due to the easy formation of short circuiting filaments, we could consistently and reproducibly compare those junctions with the Au//DPBT-PEDOT:PSS//Au diodes. As shown in Figure 3, these data are also comparable with what observed in a c-AFM diode configuration, where the top electrode is a conductive Pt coated tip. The analysis of the V_T plot, shown in figure 3, reveals that the normalized data are essentially the same. Interestingly, despite the differences in the investigation methods employed, we found the same $V_T = (0.32 \pm 0.03)$ V all across the different approaches. Such V_T is therefore the fingerprint of DPBT molecule in the conduction, no matter which junction configuration is used for the investigation. This appears as a first confirmation that the molecule rather than the diode structure is determining the junction electrical properties. Such solid persistency of an electrical parameter associated with a conjugated molecular *ensemble* probed in different junction architectures has not been previously reported. Moreover, while current density is usually not comparable in nano- and micro-pore junctions^{12a} as very often observed the current density is not scalable with the junction area, the robustness of V_T for DPBT junctions highlights a possible discriminating factor when comparing junctions characterized by very different probing areas.

As discussed above, a question arises about the possible physical origin of this parameter, V_T , in the junctions under investigation. This V_T corresponds to a clear change in conductivity of the junction, as shown by dI/dV measurement on a Au//DPBT//Au sample, directly performed with a lock-in based technique (see Supporting Information, Figure S3). However at this stage we still cannot attribute the presence of a V_T to a transition between different transport mechanisms.

Deeper insights on the transport mechanism require further investigations. A molecular length dependence study is in principle an important tool to rationalize the transport regimes,^{12a} as an exponential dependence of the conductivity with length would be compatible with a non resonant tunneling process, while a linear dependence would imply an incoherent hopping process. However DPBT offers too many possibilities for varying the molecular length, as by changing the repeating unit in the aromatic core or in the alkylic side chains, making the approach not readily viable in this case. Temperature dependent measurements at different bias voltage become therefore mandatory to clearly disentangle and address different possible transport mechanisms.

Temperature and bias dependent measurements for the Au//DPBT//Au junction are reported in Figure 4. Reversible, upward and downward temperature cycles demonstrate the stability of the junction. Analogous analysis performed on the thermal dependence of Au//DPBT-PEDOT:PSS//Au junctions (Figure 5) allows for the same conclusions and observations (see Discussion session). Independently of the underlying transport process, the substantial correspondence of the thermal dependence as found in junctions with and without PEDOT:PSS is a very critical evidence and confirms that the charge transport is not mainly ruled by the top conducting polymer or by defects following the deposition of the top Au electrode either, but rather associated with a molecular contribution.

All the data showed in Figure 4 are in the positive bias region and, due to the symmetry of the I - V curves at all temperatures, the same dependence is observed for the negative bias. Though this experimental evidence can be intuitive for the Au-SAM-Au sample, it is less straightforward to give a proper explanation for the observed symmetry in the PEDOT:PSS junctions. Similar findings have been previously reported for other molecular systems.²⁴ Possible causes for such behavior are *i*) the similar work function of the two opposite electrodes, PEDOT:PSS and Au, providing the injection of similar current densities, or *ii*) a Fermi level pinning regime.²⁵

We also compared such thermal dependence as found for DPBT junctions with those spurious phenomena which can provide thermal dependent features even in saturated alkyl chain SAMs, and whose transport has been very often shown to be coherent and non resonant. Such comparative analysis is reported in the SI, and it shows that defective alkyl thiol junctions do not present the complex temperature dependence as found for DPBT junctions.

Discussion

The temperature and bias dependent measurements of a Au//DPBT//Au junction are shown in figure 4a. The temperature dependence of the V_T is shown in figure 4b, where a broadening of the FN minima is observed with lower temperatures. For these junctions, marked temperature dependence is observed in the temperature range between 330 and 280 K (blue box figure 4a). A very weak or totally absent thermal dependence is expected in a non resonant tunneling process, while a clear thermal activation has been so far rationalized either as an effect of contact Fermi level broadening within a non resonant process or as a hopping process.^{12a} We found that this data range can be fitted with an Arrhenius dependence, returning an activation energy (E_a) which

is much higher at lower bias ($E_a \sim 85$ meV from 10 mV up to 40 mV) and progressively decreasing with increasing bias voltage and tends to lower values at higher bias (~ 0.01 - 0.02 eV above 0.4 V, figure 4c). This evidence strongly suggests that different mechanisms are responsible for the high bias and low bias regime.

While the low bias and more strongly temperature dependent regime is discussed later,²⁶ for high bias and high temperature good data fitting was found for a root square dependence of the current on temperature. Such dependence has already been reported for injection processes at inorganic/organic interfaces and follows the Richardson-Schottky model for thermoionic emission at a metal vacuum interface.²⁷ This mechanism is very well in line with the bias independent activation energy found for higher biases (> 0.4 V, figure 4c), i.e. biases higher than V_T .

From Figure 4, at T below 280 K we can clearly recognize two regions as a function of the applied bias (indicatively, green and red boxes figure 4a). Weak but measurable temperature dependence appears on the whole region from 280 K to 77 K at low biases, and an almost temperature independent region is found at higher biases. The temperature independent region above V_T can be easily assigned to a direct tunneling process which is field assisted (red box).²⁸

A less straightforward assignment can be made for the region between 240 - 77 K and 10 - 50 mV (within the green box). A very good interpolation of those data is only found for a cubic dependence of the resistance on T (Figure S5). Such dependence can be explained neither with a purely molecular mechanism, nor with a simple field assisted injection mechanism, nor with a thermionic emission. Such power dependence upon T is also responsible for the reversible broadening observed in the V_T plot (Figure 4c). We highlight that this is very likely originated by the same mechanism responsible for the similar broadening already observed by Trouborst *et*

*al.*²⁹ for pure gold break junctions in vacuum conditions and in absence of any molecular system. Therefore a molecular based mechanism cannot explain such low temperature behavior. Here we provide a possible explanation of such dependence. According to the Wiedemann-Franz law, relating the electrical conductivity with the thermal conductivity in metals, the presence of a temperature gradient between two electrodes, caused by bias applied to one electrode, determine a power law dependence of the current versus temperature (see SI for the derivation). At the base of this power law is the current dependence on the metal phonons energy, i.e. on the role they play into the electron tunneling probability. While at room temperature all the metal phonons are already active, at low temperatures the activation of thermal phonons can increase the tunneling probabilities. So far the influence of the metal phonons on the electron transport processes in organic diode studied at low temperature has been disregarded, and molecular contributions to the transport have been claimed before considering such a spurious effect.³⁰ Hence, we propose that at very low bias and low temperature, thermal effects deriving from the metal electrode contacts can control the tunneling current. In conclusion, at temperatures below 280 K, the V_T which shifts to lower values (~ 0.32 V at 200 K and ~ 0.07 V at 80 K), is associated with a transition from a metal phonons mediated transport at low biases to a non-resonant tunneling transport at higher biases.

We discuss now the transport regime at low biases between 330 K and 280 K, where marked temperature activation is found. An E_a of 85 meV is low if compared to the expected energy difference between the gold Fermi level and the HOMO of the molecule (~ 0.3 eV). According to a previously reported work, the calculated reorganization energy (λ) needed to ionize the DPBT aromatic unit in vacuum is $\lambda \sim (0.2 - 0.3)$ eV.³¹ Considering the semi-classical Marcus model for electron transfer, which would imply a hopping process, E_a would be proportional to

$\lambda/4$, which would make reasonable the low E_a value found from the slope in the Arrhenius plot. However, we cannot be conclusive at this stage regarding such process, also considering that when the molecule is bound on a solid substrate and interacts with nearest neighboring molecules in the SAM, the activation energy can be very different from what is calculated in vacuum for a single molecule and may not be simply associated to the molecular reorganizational energy. Therefore other reasons for such low energetic barrier have to be discussed first. Previous works have already reported similar activation energy (~ 0.1 eV), but mostly for fully conjugated systems embedded in a break junction³² or in a c-AFM configuration.³³ Choi *et al.*³⁴ investigated a fully conjugated molecule, and according to their interpretation the observed low activation energy has to be assigned to the intramolecular hopping process, while no energetic barrier would exist at the gold/molecule interface. Similar conclusions were drawn by Luo *et al.*,³³ who embedded multiple units of a ruthenium complex within two alkylated side chains (O-(CH₂)₆). They showed a similar low values for the activation energy, only when more than two ruthenium complexes were present, resulting in a very long molecular wire where a hopping process was more likely to occur. Sayed *et al.*³⁵ observed very low activation energy (~ 0.1 eV), for long and fully conjugated molecule in an all carbon molecular junction. The discrepancy between this value and the expected hopping energy was explained in terms of coherent tunneling process affected by a broadened Fermi function of the carbon electrode.³⁶ In particular, in order to explain their data, the authors introduced the thermal dependence of the Fermi function, as described by Simmons,^{18,37} including molecular parameters such as the SAM dielectric constant and an electron effective mass dependent upon the molecular conjugation length. Besides the difficulty to associate an electron effective mass to the short conjugated molecules under study, we note that the Simmons model cannot explain the observed dependence of the activation

energy from the bias as observed in Figure 4c. Therefore, the effect of the broadening of the Au Fermi function does not appear to be a strong enough argument for the observed temperature dependence in this case.^{12b}

Therefore our observations of temperature activation at low bias can be rationalized with a hopping process. The fact that it appears only at low biases is consistent with the short length of the molecule, which is not long enough to effectively decrease the direct tunneling between the two electrodes. However, the same molecular length is not consistent with an intramolecular hopping process, i.e. with the presence of multiple hopping sites on the molecule. Therefore the only plausible explanation supporting hopping is that the aromatic core represents a single hopping site for the charge between the two electrodes. Further experiments will be needed to fully confirm this hypothesis, e.g. by varying the chain length of the alkylic spacers. We also notice that a pinning mechanism is also compatible with a hopping mechanism. The presence of the short insulating alkyl chains and the proximity of energy levels between the Fermi energy level of gold ($E_{F,\text{gold}}$) and the HOMO of DPBT could favor a metal-molecule coupling leading to molecular electron density redistributions. The formation of hybrid states, as also foreseen in pinning mechanism, can also explain the observed low activation energy.^{25,38}

Given the difficulty in assessing a tunneling mechanism according to the Simmons model, in all the other mechanisms described above both the molecules and the electrodes have to be considered to explain the observed data at low bias and close to room temperature, implying a resonant transport mechanism. So far in the literature there are no clear reports of an electrode molecule coupling despite the presence of insulating alkyl chains in short molecular wires.

Conclusions

The thorough comparison of various junctions' architectures demonstrates that the ubiquitous $V_T = (0.32 \pm 0.05)$ eV found for DPBT based junctions is a signature of the molecular role in the charge transport. Temperature and bias dependent measurements allow the identification of different transport regimes. The substantial agreement between temperature dependent conduction in junctions with Au and PEDOT:PSS top electrode rules out the possibility of trivial spurious effects (e.g. metal filaments) inducing such temperature dependence. We showed that at low bias and close to ambient temperature a resonant transport ($E_a = 85$ meV) is possible for short and not fully conjugated molecules. This mechanism is compatible with the presence of a single localized state, strongly contributed by the aromatic core of the molecule, to which charge injected from electrodes can hop to. In this frame, in agreement with recent studies on molecular junctions,^{19a,21} we can exclude that for DPBT junctions V_T discriminates between direct and FN tunneling; instead, we show that for biases exceeding V_T and close to room temperature, a transition from a resonant to a thermionic emission takes place.³⁹

In the low temperature range other two mechanisms are present. For biases exceeding V_T a thermal independent, tunneling regime is clearly evidenced. Interestingly, at low temperatures and low biases, we found that thermal conductivity determines a power dependence of the current on temperature though a tunneling mechanism is still occurring in the junction. We have associated such regime to the influence of metal-phonons, spurious, i.e. non involving molecular electronic levels, contribution to the junction transport.

While statistical measurements are to date one of the most reasonable approaches for studying molecular junctions, we would emphasize on the importance of temperature dependence studies in order to gather more awareness on the multiple channels which might

contribute to the junction transport, in particular of those non molecular mechanism which might mislead the interpretation.

The overall importance of our work relies both in highlighting the robustness of an electrical parameter such as V_T with respect to the variation in junction architecture and probing area, and in the definition of those fundamental parameters, energy level proximity to the electrode work function and alkyl chain length, which can control the resonant transport in molecular junctions with a conjugated core. Resonant processes are mostly desirable as they would bring-in the particular signature of the chosen molecules making worthwhile the specific effort into design and synthesis.

Methods

The ω -alkylthiol functionalized 3,3'-diphenyl 2,2'-bithiophene (DPBT) has been synthesized according to a previously reported route.⁴⁰

A scheme of the diode junction studied in this work is presented in Figure 1. The diode junction has been prepared by vacuum evaporation of 70 nm of gold onto 1737F glass slides. A ~ 1.3 μm thick photoresist layer (S1813) was spun on the gold substrate. Subsequently, part of the photoresist was removed through a photolithographic process, providing a patterning with 5-10-20-40-80 μm diameter holes. After oxygen plasma treatment (100 W, 10 min), the substrates were immersed overnight in a 5×10^{-4} M solution of DPBT in toluene. After vigorous rinsing with chloroform and drying under N_2 , the samples were either directly placed into the evaporator chamber for the gold top electrode deposition or topped with a PEDOT:PSS layer. In the last

case, the PEDOT:PSS interlayer was deposited by spin-coating on top of the molecular assembly prior to gold electrode evaporation.

Variable temperature I - V measurements have been performed by means of an Agilent B1500 Semiconductor Parameter Analyzer in a cryogenic probe-station (Janis). The temperature value was monitored with 4 sensors placed in different position of the chamber. To allow for a good thermal contact between the heat exchanger and the sample, the substrate was attached to the sample holder through a thermal paste (ApiezonN). The temperature at the top surface of the sample was also monitored in control experiments by recording the temperature of an additional Si diode sensor placed on top of a dummy 1737F glass substrate of the same thickness and comparable lateral dimensions of the actual samples.

Direct measurements of the first derivative of the I - V curves were performed by providing a DC bias with a superimposed AC 10 mV at 654 Hz through a Keithley 3390 signal generator, and by reading the output AC signal at 654 Hz, amplified with a transimpedance amplifier (DHPCA-100, FEMTO Messtechnik GmbH), on a lock-in amplifier (SRS830, Stanford Research Systems). Conductivity measurements were performed at 77K.

I - V characteristics have also been measured on a DPBT SAM chemisorbed on clean gold surface through a Conductive Probe Atomic Force Microscopy (c-AFM, 5500 Agilent Technology). Gold substrates used for c-AFM junctions experiment were prepared by evaporating 1.5 nm of Cr on mica prior the evaporation of 20 nm thick layer of gold. This allows us to obtain substrate with a roughness of ~ 1.5 nm. Conductive platinum-coated silicon nitride cantilevers (N9540-60002, Agilent Technologies, Santa Clara, CA) with a nominal force constant of 6 N/m were used for c-AFM measurements. Measurements were carried under nitrogen atmosphere. We observed that I - V characteristics measured with c-AFM are dependent upon the force constant of

the chosen tip, with higher tip forces being responsible for SAM penetration and formation of short circuits.⁴¹

FIGURES

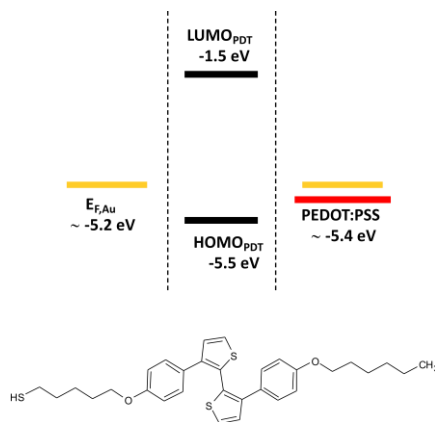


Figure 1: Left: molecular structure of 3-(4-hexyloxyphenyl)-3'-(4-(6-mercapto)hexyloxyphenyl)-2,2'-bithiophene (DPBT); Right: scheme of energy levels.

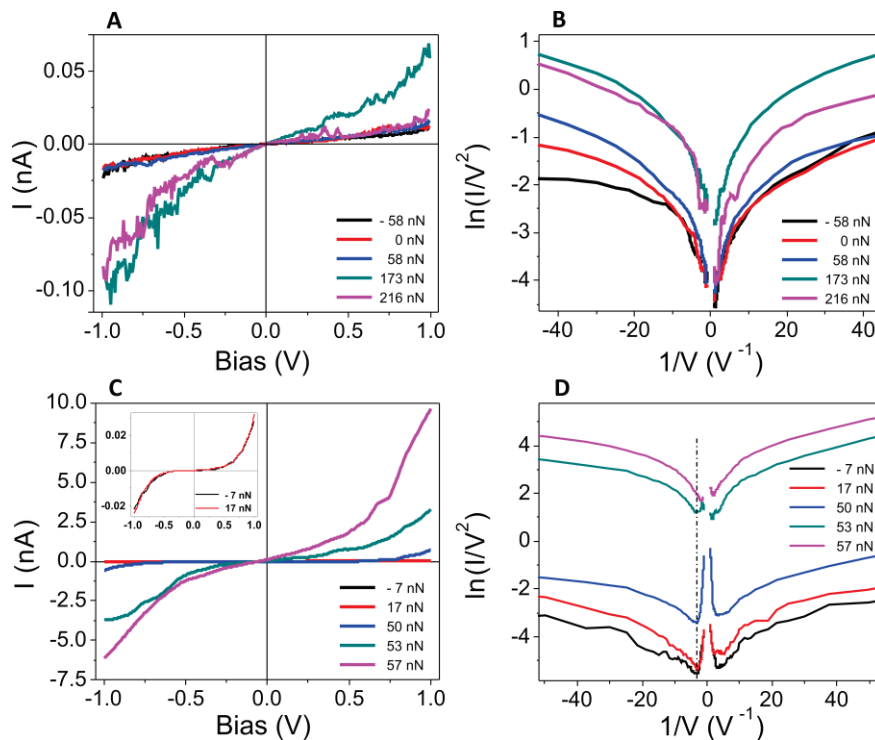


Figure 2: A-B: I - V plot (A) and transition voltage plot (B) acquired on a c-AFM junction configuration for C14 SAM on gold; C-D: I - V plot (C) and transition voltage plot (D) acquired on a c-AFM junction

configuration for DPBT SAM on gold. The inset in C shows the I - V plot acquired for the lowest applied tip loads. Lower loads correspond to the minimum load required to achieve an electrical contact with the SAM/Au substrate. At higher loads, short circuits are very likely to occur, producing increased current densities especially in the case of non-densely packed monolayers. However, in densely packed and insulating SAMs, as for the C14 SAM, increasing the tip-load implies a higher probability to contaminate the metallic tip with detachment and physisorption of the SAM molecules on the tip. Such case can lead to the formation of a more insulating tip at increasing load with consequent decrease of the measured current as we can see by comparing the I - V curve acquired for C14 SAM at 173 nN and 216 nN. The abrupt jump in conductance observed for C14 (above 58 nN) and for DPBT (above 53 nN) is likely associated to a tip breaking the SAM packing, therefore reducing the gold substrate-tip distance, resulting also in a clear modification of V_T .

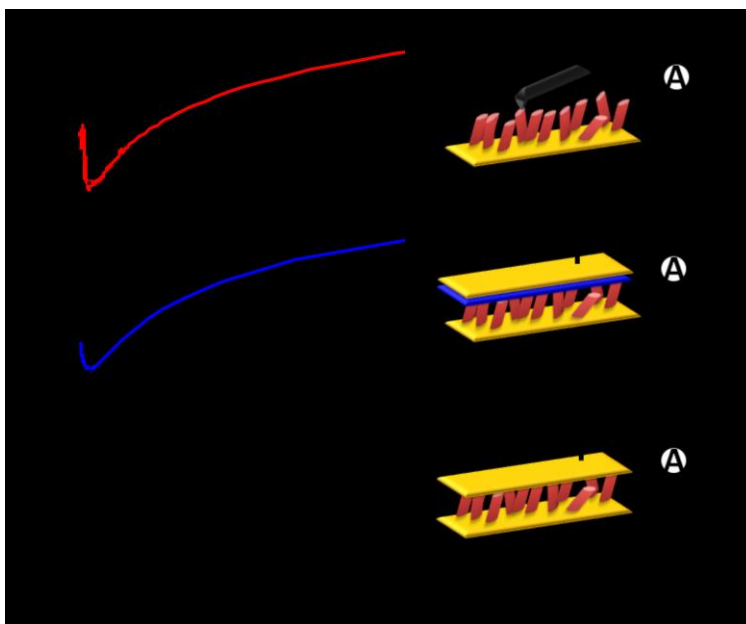


Figure 3: Transition voltage plot of the measured I - V characteristics in the three diodes configuration. a) c-AFM junction, b) PEDOT:PSS diode junction, c) Au junction. The dashed line is a guide to the eye showing the position of V_T .

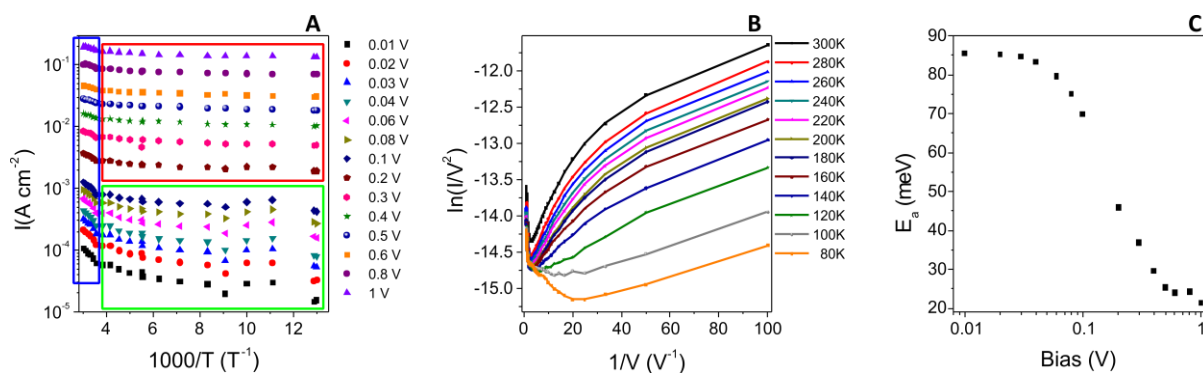


Figure 4: a: current dependence on temperature and bias for a Au-DPBT-Au junction (reversible up-down cycles at 180 K and 77 K show the stability of the measured junction); b: broadening of the transition voltage plot at lowering temperatures (Au-DPBT-Au); c: Bias dependence of the activation energy as extracted from the Arrhenius plot of the current vs temperature (T) for $330 < T < 280$.

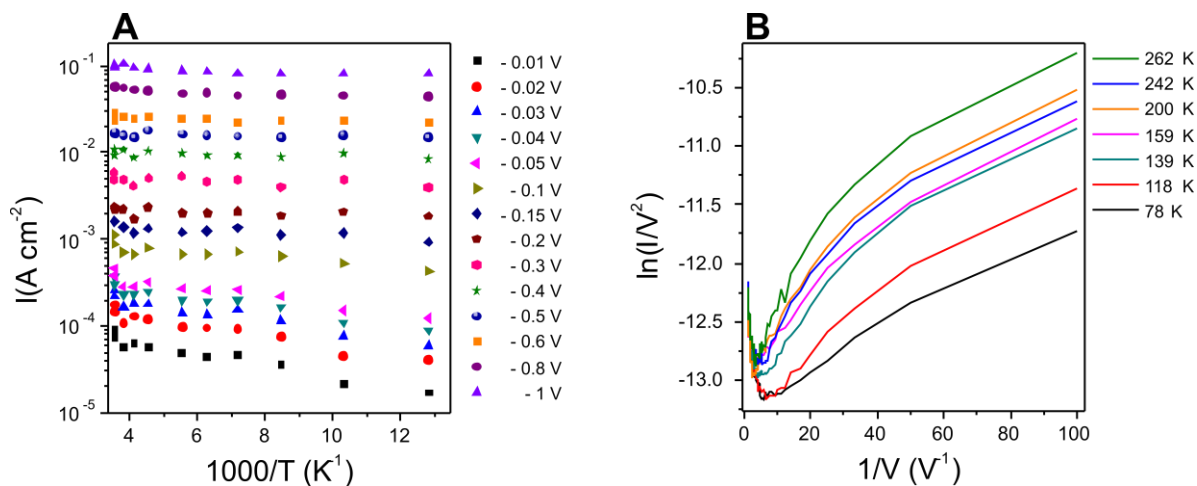


Figure 5: A: Current dependence on temperature and bias for a Au-DPBT-PEDOT:PSS-Au junction. B: Transition voltage plot Au-DPBT-PEDOT:PSS-Au junction.

References

- (1) (a) Song, H.; Reed, M. A.; Lee, T. *Adv Mater* **2011**, *23*, 1583(b) Metzger, R. M.; Mattern, D. L. *Top Curr Chem* **2012**, *313*, 39.
- (2) (a) Pace, G.; Ferri, V.; Grave, C.; Elbing, M.; von Hanisch, C.; Zharnikov, M.; Mayor, M.; Rampi, M. A.; Samori, P. *P Natl Acad Sci USA* **2007**, *104*, 9937(b) Pace, G.; Petitjean, A.; Lalloz-Vogel, M. N.; Harrowfield, J.; Lehn, J. M.; Samori, P. *Angew Chem Int Edit* **2008**, *47*, 2484.
- (3) Mativetsky, J. M.; Pace, G.; Elbing, M.; Rampi, M. A.; Mayor, M.; Samori, P. *J Am Chem Soc* **2008**, *130*, 9192.
- (4) (a) Chang, S.; He, J.; Zhang, P. M.; Gyarfás, B.; Lindsay, S. *J Am Chem Soc* **2011**, *133*, 14267(b) Guedon, C. M.; Valkenier, H.; Markussen, T.; Thygesen, K. S.; Hummelen, J. C.; van der Molen, S. *J. Nat Nanotechnol* **2012**, *7*, 304(c) Aradhya, S. V.; Frei, M.; Hybertsen, M. S.; Venkataraman, L. *Nat Mater* **2012**, *11*, 872.
- (5) (a) Perrin, M. L.; Verzijl, C. J. O.; Martin, C. A.; Shaikh, A. J.; Eelkema, R.; van Esch, J. H.; van Ruitenbeek, J. M.; Thijssen, J. M.; van der Zant, H. S. J.; Dulic, D. *Nat Nanotechnol* **2013**, *8*, 282(b) Reed, M. A.; Zhou, C.; Muller, C. J.; Burgin, T. P.; Tour, J. M. *Science* **1997**, *278*, 252.
- (6) (a) Zhou, C.; Deshpande, M. R.; Reed, M. A.; Jones, L.; Tour, J. M. *Appl Phys Lett* **1997**, *71*, 611(b) Park, S.; Wang, G.; Cho, B.; Kim, Y.; Song, S.; Ji, Y.; Yoon, M. H.; Lee, T. *Nat Nanotechnol* **2012**, *7*, 438.
- (7) Yang, Y. C.; Gao, P.; Gaba, S.; Chang, T.; Pan, X. Q.; Lu, W. *Nat Commun* **2012**, *3*.
- (8) Bergren, A. J.; Harris, K. D.; Deng, F. J.; McCreery, R. L. *J Phys-Condens Mat* **2008**, *20*.
- (9) (a) Bonifas, A. P.; McCreery, R. L. *Nat Nanotechnol* **2010**, *5*, 612(b) Alexander B. Neuhausen, A. H., Joseph A. Sulpizio, Christopher E. D. Chidsey, and David Goldhaber-Gordon *Acs Nano* **2012**, *11*, 9920.
- (10) (a) Akkerman, H. B.; Naber, R. C. G.; Jongbloed, B.; van Hal, P. A.; Blom, P. W. M.; de Leeuw, D. M.; de Boer, B. *P Natl Acad Sci USA* **2007**, *104*, 11161(b) Neuhausen, A. B.; Hosseini, A.; Sulpizio, J. A.; Chidsey, C. E. D.; Goldhaber-Gordon, D. *Acs Nano* **2012**, *6*, 9920.
- (11) (a) Min, M.; Seo, S.; Lee, S. M.; Lee, H. *Adv Mater* **2013**(b) Seo, S.; Min, M.; Lee, J.; Lee, T.; Choi, S. Y.; Lee, H. *Angew Chem Int Edit* **2012**, *51*, 108.
- (12) (a) Luo, L. A.; Choi, S. H.; Frisbie, C. D. *Chem Mater* **2011**, *23*, 631(b) Sayed, S. Y.; Fereiro, J. A.; Yan, H. J.; McCreery, R. L.; Bergren, A. J. *P Natl Acad Sci USA* **2012**, *109*, 11498(c) McCreery, R. L.; Yan, H. J.; Bergren, A. J. *Phys Chem Chem Phys* **2013**, *15*, 1065.
- (13) McCreery, R. L. *Chem Mater* **2004**, *16*, 4477.
- (14) (a) Choi, S. H.; Kim, B.; Frisbie, C. D. *Science* **2008**, *320*, 1482(b) Randall H. Goldsmith, O. D., Thea M. Wilson, Daniel Finkelstein-Shapiro, Mark A. Ratner and Michael R. Wasielewski *Journal of American Chemical Society* **2010**, *132*, 11658.
- (15) Beebe, J. M.; Kim, B.; Frisbie, C. D.; Kushmerick, J. G. *Acs Nano* **2008**, *2*, 827.
- (16) Engelkes, V. B.; Beebe, J. M.; Frisbie, C. D. *J Phys Chem B* **2005**, *109*, 16801.
- (17) Beebe, J. M.; Kim, B.; Gadzuk, J. W.; Frisbie, C. D.; Kushmerick, J. G. *Phys Rev Lett* **2006**, *97*.
- (18) Simmons, J. G. *J Appl Phys* **1964**, *35*, 2655.
- (19) (a) Baldea, I. *Chem Phys* **2012**, *400*, 65(b) Bâldea, I. *RSC Advances* **2014**, *4*, 33257.
- (20) Fatemeh Mirjani, J. M. T., Sense Jan van der Molen *Physical Review B* **2011**, *84*, 115402.
- (21) Vilan, A.; Cahen, D.; Kraisler, E. *Acs Nano* **2013**, *7*, 695.
- (22) Wang, G.; Kim, T. W.; Jo, G.; Lee, T. *J Am Chem Soc* **2009**, *131*, 5980.
- (23) Lennartz, M. C.; Atodiressei, N.; Caciuc, V.; Karthäuser, S. *J Phys Chem C* **2011**, *115*, 15025.
- (24) (a) Kronemeijer, A. J.; Katsouras, I.; Huisman, E. H.; van Hal, P. A.; Geuns, T. C. T.; Blom, P. W. M.; de Leeuw, D. M. *Small* **2011**, *7*, 1593(b) Kronemeijer, A. J.; Akkerman, H. B.; Kudernac, T.; van

- Wees, B. J.; Feringa, B. L.; Blom, P. W. M.; de Boer, B. *Adv Mater* **2008**, *20*, 1467(c) Wang, G.; Na, S. I.; Kim, T. W.; Kim, Y.; Park, S.; Lee, T. *Org Electron* **2012**, *13*, 771.
- (25) (a) Van Dyck, C.; Geskin, V.; Cornil, J. *Advanced Functional Materials* **2014**(b) Braun, S.; Salaneck, W. R.; Fahlman, M. *Adv Mater* **2009**, *21*, 1450.
- (26) Worne, J. H.; Anthony, J. E.; Natelson, D. *Appl Phys Lett* **2010**, *96*.
- (27) Scott, J. C. *J. Vac. Sci. Technol. A* **2003**, *21*, 521.
- (28) (a) Scott, J. C.; Malliaras, G. G. *Chem. Phys. Lett.* **1999**, *299*, 115(b) Ng, T. N.; Silveira, W. R.; Marohn, J. A. *Phys. Rev. Lett.* **2007**, *98*.
- (29) Trouwborst, M. L.; Martin, C. A.; Smit, R. H. M.; Guedon, C. M.; Baart, T. A.; van der Molen, S. J.; van Ruitenbeek, J. M. *Nano Lett* **2011**, *11*, 614.
- (30) Asadi, K.; Kronemeijer, A. J.; Cramer, T.; Koster, L. J. A.; Blom, P. W. M.; de Leeuw, D. M. *Nat Commun* **2013**, *4*.
- (31) Fazzi, D.; Castiglioni, C.; Negri, F.; Bertarelli, C.; Famulari, A.; Meille, S. V.; Zerbi, G. *J Phys Chem C* **2008**, *112*, 18628.
- (32) Yoram Selzer, M. A. C., Theresa S. Mayer, and David L. Allara *Journal of American Chemical Society* **2004**, *126*, 4052.
- (33) Luo, L.; Benameur, A.; Brignou, P.; Choi, S. H.; Rigaut, S.; Frisbie, C. D. *J Phys Chem C* **2011**, *115*, 19955.
- (34) Choi, S. H.; Risko, C.; Delgado, M. C. R.; Kim, B.; Bredas, J. L.; Frisbie, C. D. *J Am Chem Soc* **2010**, *132*, 4358.
- (35) Sayed Youssef Sayed, A. B., Mykola Kondratenko, Yann Leroux, Philippe Hapiot, and Richard L. McCreery *Journal of American Chemical Society* **2013**, *135*, 12972.
- (36) Yan, H. J.; Bergren, A. J.; McCreery, R.; Della Rocca, M. L.; Martin, P.; Lafarge, P.; Lacroix, J. C. *P Natl Acad Sci USA* **2013**, *110*, 5326.
- (37) Bergren, A. J.; McCreery, R. L.; Stoyanov, S. R.; Gusarov, S.; Kovalenko, A. *J Phys Chem C* **2010**, *114*, 15806.
- (38) Heimel, G.; Duhm, S.; Salzmann, I.; Gerlach, A.; Strozecka, A.; Niederhausen, J.; Burker, C.; Hosokai, T.; Fernandez-Torrente, I.; Schulze, G.; Winkler, S.; Wilke, A.; Schlesinger, R.; Frisch, J.; Broker, B.; Vollmer, A.; Detlefs, B.; Pflaum, J.; Kera, S.; Franke, K. J.; Ueno, N.; Pascual, J. I.; Schreiber, F.; Koch, N. *Nat Chem* **2013**, *5*, 187.
- (39) (a) Pakoulev, A. V.; Burtman, V. *J Phys Chem C* **2009**, *113*, 21413(b) Li, J. C.; Wang, D.; Ba, D. C. *J Phys Chem C* **2012**, *116*, 10986.
- (40) Canesi, E. V.; Bertarelli, C. *Phosphorus, Sulfur, and Silicon and the Related Elements* **2011**, *186*, 1298.
- (41) (a) Jianwei Zhao, J. J. D. *Nanotechnology* **2003**, *14*, 1023(b) Frisbie, D. J. W. a. C. D. *Journal of American Chemical Society* **2001**, *123*, 5549.